PREPARATION OF THIN FILMS YSZ+PLATINUM BY DIP COATING AND THEIR CHARACTERIZATION IN JUNCTIONS FOR OXYGEN DETECTION

DIMITRE DIMITROV, SALZITZA ANASTASOVA, CECO DUSHKIN

Department of General and Inorganic Chemistry,
Faculty of Chemistry

Димитър Димитров, Сълзица Анастасова, Цецо Душкин. ПОЛУЧАВАНЕ НА ТЪНКИ ФИЛМИ ОТ YSZ+ПЛАТИНА ВЪРХУ ТВЪРДА ПОДЛОЖКА ЧРЕЗ ИЗТЕГЛЯНЕ ОТ СУСПЕНЗИЯ И ТЯХНОТО ХАРАКТЕРИЗИРАНЕ КАТО КОНТАКТИ ЗА ДЕТЕКТИРАНЕ НА КИСЛОРОД

Изследвана е възможността за импрегниране на итриево-стабилизиран циркониев диоксид (YSZ) с платинови наночастици. Предварително синтезираните платинени наночастици се вкарват в тънки филми от YSZ, нанесени върху твърда подложка чрез изтегляне от суспензия. Филмите от YSZ+Pt с 5.2 mol% платина са тествани за регистриране на кислород като контакти от два електрода: (i) YSZ+Pt(отдолу)/YSZ(отгоре) и (ii) YSZ(отдолу)/YSZ+Pt(отгоре). Установено е, че в отсъствие на кислород потенциалната разлика на тези слоеве се увеличава по абсолютна стойност с нарастване на температурата и достига стойност на насищане при около –100 mV в случай (i) и +100 mV в случай (ii). Температурната зависимост е обяснена количествено на базата на проста моделна функция, описваща потенциалната разлика, което позволява сравняването на различни контакти при последователни тестове. В динамични условия потенциалната разлика расте (по абсолютна стойност) по време на притока на кислород (21 % във въздуха), достигайки насищане за няколко минути, а след това намалява, когато газовият поток се превключва към чист азот.

Dimitre Dimitrov, Salzitza Anastasova, Ceco Dushkin. PREPARATION OF THIN FILMS YSZ+PLATINUM BY DIP COATING AND THEIR CHARACTERIZATION IN JUNCTIONS FOR OXYGEN DETECTION

The possibility of impregnation of yttria-stabilized zirconia (YSZ) with platinum nanoparticles is studied. The pre-synthesized platinum nanoparticles are embedded in YSZ thin films deposited on a solid substrate by the dip-coating method. The YSZ+Pt films with 5.25 mol% of platinum are tested for oxygen detection as junctions of two electrodes: (i) YSZ+Pt(bottom)/YSZ(top) and (ii) YSZ(bottom)/YSZ+Pt(top). It is found that at no oxygen the potential difference of these junctions is increasing in absolute value with the temperature reaching a saturation value of about –100 mV for case (i) and +100 mV for case (ii). Quantitative understanding of the temperature behaviour is received based on a simple model function for the potential difference, which allows comparison of various junctions at successive tests. In dynamic conditions the potential difference is increasing (in absolute value) during the inflow of oxygen (21 % in air) reaching saturation within a couple of minutes and then decreasing when the gas flow is switched to pure nitrogen.

Keywords: YSZ thin films; platinum nanoparticles; sol-gel preparation; dip-coating; potentiometric oxygen sensor

PACS number: 81.05.Je

1. INTRODUCTION

Oxygen sensors based on yttria-stabilized zirconia (YSZ) have been largely used in various applications during the last twenty years. The major applications are in combustion environments of industrial furnaces and automobile exhausts, semiconductor manufacturing, biotechnology and food processing, laboratory and physiological applications (e.g. life support systems and home health-care systems). The oxygen sensor is used also for detection of neutral atomic oxygen at typical low Earth orbit altitudes, which is important for spacecraft designers and manufactures. Although various kinds of both amperometric and potentiometric sensors are currently available, innovation in the form of more miniaturized and cheaper oxygen sensor are of important consideration. Important is also the reducing of power consumption of the sensor and the increasing of long-term reliability by reducing its working temperatures. There are also trends to simplify the construction of the oxygen sensor by avoiding classical two-compartment tubular geometry where the inside compartment is usually exposed to air that serves as the reference electrode for fixed and known oxygen activity, while the outer-side electrode senses the unknown oxygen content in the environment. In this situation the most suitable

device is probably that based on the YSZ thin films. That is why it is important to produce YSZ thin films with desirable properties, which could be used in the thin-film oxygen sensor. The authors of [1] investigated the cathodic behaviour of the sputtered platinum on 4-mol% Y_2O_3-ZrO_2 composite electrode by means of d.c. measurements in the temperature range 450-800 °C under wide range of oxygen concentrations. This was done in order to reduce the morphological changes with the high temperature annealing, but to maintain the long-term stability of the gas sensor. In this case the Y_2O_3-ZrO_2 thin films of 0.1 to 1.0 μm thick were prepared on the 0.45 to 0.5 μm thick Pt film. A silicon-based YSZ amperometric oxygen sensor with a cross-bridge structure had been developed in [2]. The YSZ film of thickness 4000 Å was deposited by sputtering. Its sensing area of 380×240 μm is a substantial reduction in size from the common sensors. Based on silicon wafer, the authors of [3] developed by micro-fabrication a miniaturized potentiometric oxygen sensors connected in series. In this case, YSZ thin film of thickness 1 μm was deposited by reactive d.c. sputtering using argon-oxygen atmosphere for an yttrium doped zirconium target. In a thin-film limiting-current-type oxygen sensor [4] the graded-composition layers were formed by co-sputtering of platinum and yttria-stabilized zirconia (YSZ) electrolyte materials. Sputter-deposited YSZ thin-films on silicon substrate are also reported in [5].

In a previous work [6], YSZ thin films containing platinum nanoparticles were deposited by spay pyrolysis. The principles of detection of oxygen by these sensing media has been investigated with respect to the effect of the platinum nanoparticles on the electrical conductivity and oxygen transportation properties of YSZ thin films [7]. Our observations are in accord with ref. [8], where it is stated that the addition of a metal to the ceramic matrix often produces a composite with more desirable properties than the individual components (YSZ). These authors impregnated sonochemically synthesized Pt nanoparticles (of diameters of about 2 nm) into zirconia nano-grains (20-45 nm). Further, other authors [9] used YSZ supported platinum catalysts (YSZ+Pt) for the reforming of CH_4/CO_2. The YSZ+Pt catalysts were prepared by the incipient impregnation of YSZ ceramics with water solution of $H_2PtCl_6.6H_2O$ followed by a thermal treatment. By this way they achieved enhanced adsorption, activation and dissociation of CO_2 on the YSZ grains. The other ways of impregnation of YSZ matrix with platinum are described in [10]. Two impregnation methods were applied: (i) immersion of porous YSZ into a Pt salt solution followed by reduction of the platinum salt and (ii) deposition of Pt in porous YSZ at an electrode by electrolysis. The results were enhancement in the capacitance of YSZ ceramic capacitors.

The first study on the application of Pt nanoparticles in oxygen sensors is given in ref. [11]. These authors elaborated an amperometric oxygen sensor containing a composite Pt+YSZ layer. This layer is deposited on a bulk YSZ material with an overall thickness of 2–3 mm comprising pressed and sintered ceramic grains of a typical size of 1–1.5 μm. The platinum forms submicron particles of average diameter of 0.1–0.6 μm depending on the method of synthesis. The finer particles (~100 nm in diameters) were obtained using sol-gel synthesis of the platinum powder. The fabricated sensor exhibited well-defined currents for oxygen concentrations up to 6% and the current response linearly depending on the concentration. There are two main differences between that work and the sensor outlined by us below: (i) the Pt+YSZ layer is simply used as a diffusion barrier facilitating the transportation and detection of oxygen by a thick YSZ layer (rather than as an independent thin-film electrode as in our case); (ii) the sizes of Pt particles are in the submicron domain (rather than in the nano-domain as in our case). The observed differences necessitate also a different procedure of YSZ thin film fabrication which is the dip coating from a colloidal sol in our work. Finally, this results in a junction of two thin films on a solid substrate: YSZ film and YSZ+Pt film, which exhibits a novel sensing ability with respect of oxygen.

The purpose of our research here is to develop the way of preparation of junctions containing one film of YSZ+Pt in a contact with another film of YSZ by the dip coating from a sol-gel dispersion. This necessarily leads to the impregnation of the YSZ film with Pt nanoparticles at a certain concentration of platinum. The reliability of so-prepared Pt-doped YSZ thin film is checked by applying it as the electrode in junctions (sensors) used for the detection of oxygen. It is found that they account for the oxygen concentration in the environment.

2. EXPERIMENT

2.1. FABRICATION OF JUNCTIONS CONTAINING YSZ+PT FILM

Figure 1 shows a structure of oxygen sensor, fabricated by us, with the bottom layer playing the role of an internal reference and the top layer being the working electrode. Each junction is deposited on a substrate of Rubalit® 710 with sizes 10×20 mm. The area of overlap of the two electrodes is about 7 mm in length. For preparation of the supported pure YSZ films we used sol-gel process developed by the authors of [12] as the most practical method for fab-

rication of crack-free YSZ membranes. The colloidal platinum nanoparticles are produced following the classical method of reduction of metal salt in an aqueous solution at a room temperature [13–16]. The dip-coating is performed on the apparatus described previously [17].

Let us summarize the main steps of the sol-gel technique used to prepare the junctions from Fig. 1. First we prepare solution of 11.7 g (0.025 mol) zirconium n-propoxide in isopropanol. Then a mixture of distilled water (90 ml) and isopropanol (50 ml) is added to the sol to hydrolyze the zirconia at a temperature of 90 °C. The zirconia cake is further condensed by filtration by vacuum suction. After that the cake is washed with water several times to remove the isopropanol. The residual zirconia cake is then diluted in 100 ml of water and peptized at 90-100°C overnight in the presence of 12.5 ml of 1M HNO_3. The zirconia sol, ultrasonically treated for 30 min, is mixed with polyvinyl alcohol solution (1.01 g of PVA plus 32.06 ml of water plus 1.69 ml of 1M HNO_3). 0.07 M yttrium nitrate solution is made by mixing 0.831 g of $Y(NO_3)_3.6H_2O$ with 29.24 ml of water and 1.54 ml of 1 M HNO_3. Mixing the zirconia sol with the yttrium solution, we obtain 8 mol% of yttria in the zirconia. Into the stable yttrium doped zirconia sol we add certain amount of platinum nanoparticles. They are prepared in a solution of 0.625 g of K_2PtCl_4 and 0.11 g of Na_3PO_4 in 15.1 ml of water. Argon has been blown for 20 min through the solution for oxygen removal. Then the platinum salt has been reduced by rigorous bubbling hydrogen in this solution for 10 min and left for overnight. Finally, the obtained nanoparticles suspension is added to the yttria-zirconia sol. In such a way the concentration of platinum becomes 5.25 mol% with respect to YSZ-content in the sol.

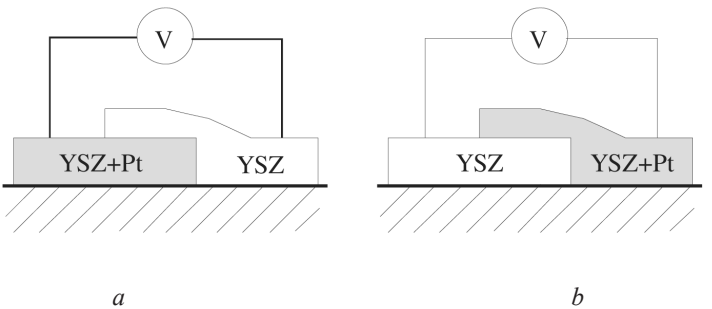

Fig.1. Sketch of the thin film junctions of YSZ and YSZ+Pt in contact: *a*) YSZ+Pt/YSZ; *b*) YSZ/YSZ+Pt

The junction thin films of YSZ and YSZ+Pt are deposited from the respective sols with deep-coating procedure. The dipping rate is 0.45 mm/s; seven dipping cycles are performed for each sample. After preparation, each YSZ or YSZ+Pt layer is calcined at 450 °C for 90 min.

The sensor structure, morphology and nanoparticles condition is investigated by Scanning Electron Microscope, SEM (JEOL, JSM 5510, Japan).

2.2. TEST OF THE JUNCTIONS

The effect of oxygen concentration in the environment on the potential difference between the overlapped layers is investigated using our home-built experimental setup described in our previous work [7]. The sensor is positioned on a ceramic holder within a quartz tube, which is situated in an electric tube furnace for regulating the working temperature of the sensor. Two needle electrodes (thermo-resistive wires of diameter of 0.75 mm) are pressed to the upper part of the sample, each one to above 1-2 mm from the overlap between the layers. By this we ensure control of the potential difference between the pure YSZ and Pt doped YSZ layers at certain temperature under oxygen exposure. The bottom layer is always connected as a common electrode, whereas the potential difference of the upper layer relatively to it is measured. For this purpose a digital voltmeter is used, which is connected to the thermo-resistive conductors, coming from the sample. For measuring the potential difference of the samples in oxygen media dry air (ca. 21 % of oxygen) is pumped in the system by using an aquarium pump. In this case the inflow is for 10 min until the value of the potential difference between the layers becomes stable. For oxygen free medium pure nitrogen from a nitrogen bottle is flown for 20 min. Two types of measurements are carried out: (i) dependence of the potential difference on the junction temperature at steady state conditions (flowing nitrogen); (ii) relaxation of the potential difference with the time to its saturation value at a fixed working temperature (alternative change from flowing air to nitrogen).

3. RESULTS AND DISCUSSION

3.1. SCANNING ELECTRON MICROSCOPY

The SEM micrograph of the Pt doped ceramics film is shown at Fig. 2 in the overlap between the YSZ and YSZ+Pt layer. At low magnification one can see the transition from pure YSZ ceramics (the dark corner to the left in Fig.

2*a*) to Pt containing ceramics. The big grains of YSZ are clearly seen as the geometrical figures of various shapes in Fig. 2*b* ranging in size between 0.5 and 1.5 μm. The Pt nanoparticles, seen as the bright spots in Fig. 2*c*,

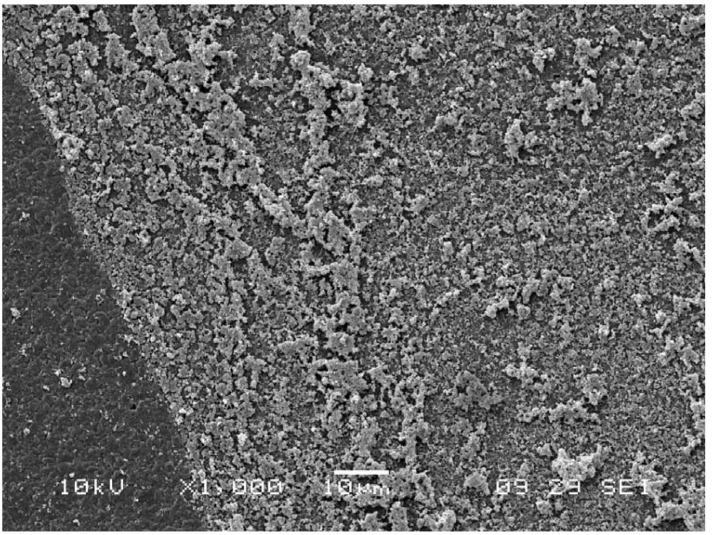

a

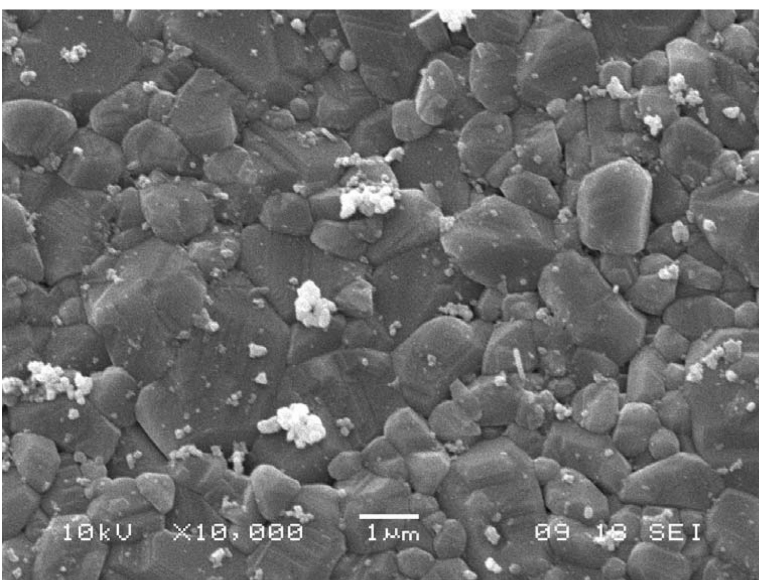

b

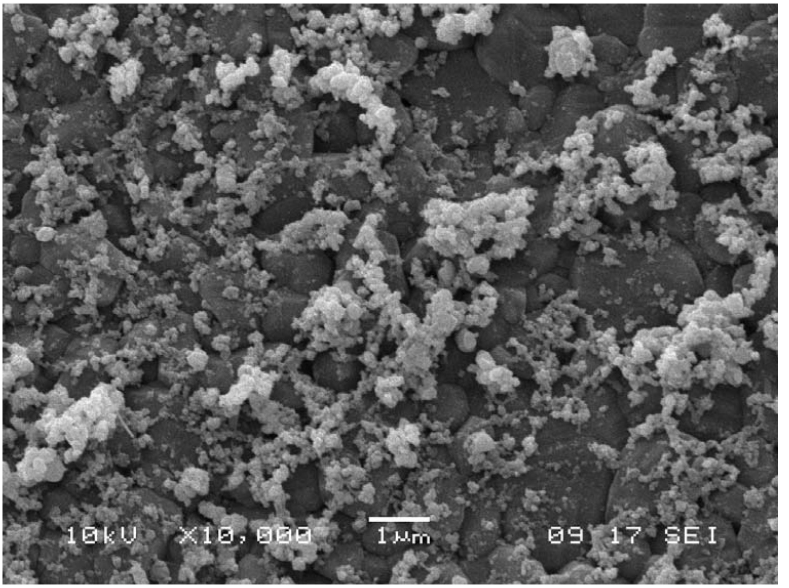

c

Fig. 2. SEM micrographs of the junction layers: *a*) transition layer YSZ+Pt(right)/YSZ(left); *b*) YSZ layer from the junction YSZ/YSZ+Pt; *c*) YSZ+Pt layer from the junction YSZ/YSZ+Pt

seem either dispersed among them or partially immersed in the grains. The Pt nanoparticles are smaller than ~100 nm although they aggregate. They are a little bit larger in comparison with the Pt nanoparticles in the grains of YST+Pt layers obtained by us by spray pyrolysis that range from 15 to 25 nm. This fact can be explained with the aggregation of Pt nanoparticles located in the interstitial volume of YSZ during the dip coating process and subsequent annealing. In contrast, the Pt nanoparticles from spray pyrolysis form in the YSZ grains in the course of sputtering.

3.2. TEMPERATURE DEPENDENCE OF THE POTENTIAL DIFFERENCE

Temperature dependence of the potential difference of YSZ+Pt/YSZ junction is shown on the Fig. 3*a*. Each successive measurement is taken during one day: about 7 hours for the entire temperature dependence. Since the platinum nanoparticles doped layer is on the bottom part of the junction (Fig. 1*a*), this part should become positively charged relative to the upper layer. Then the upper layer (pure YSZ) is negatively charged with respect to the common electrode (the bottom layer), because adding Pt nanospecies to the YSZ increases

somehow the n-type conductivity (see below). For this reason the potential difference U, measured for this junction (Fig. 3*a*) is also negative.

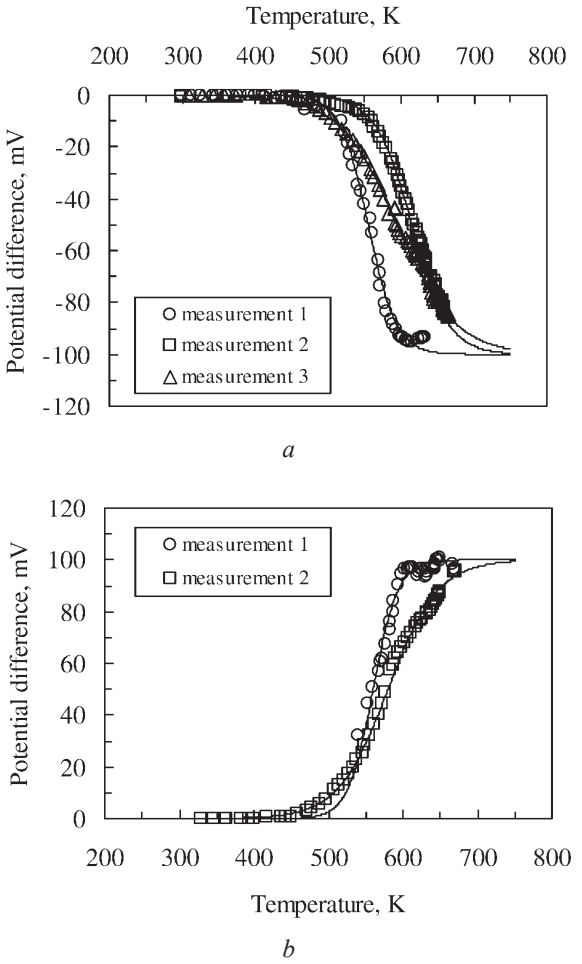

Fig. 3. Temperature dependence of the potential difference $U(T)$ in a pure nitrogen atmosphere (zero oxygen) for: *a*) YSZ+Pt/YSZ junction; *b*) YSZ/YSZ+Pt junction. The solid lines are data fits drawn by Eq. (1)

In contrast, the potential difference becomes positive for the YSZ/YSZ+Pt junction shown in Fig. 3*b*. Here the situation is opposite to the first case because the top electrode is platinum doped layer (Fig. 1*b*).

Quantitatively, U can be represented in both cases considered above as the following model function:

$$U = \frac{U_\infty}{1 + e^{\theta(\bar{T}-T)}}. \quad (1)$$

Here U_∞ is the saturation potential at infinite temperature ($T >> \bar{T}$); $\bar{T}$ is the mean of the interval of working temperatures; θ is a reciprocal temperature determining the slope of the curve (more details for Eq. (1) will be given elsewhere). The fits of the experimental data in Fig. 3 with Eq. (1) show the following trends. First, the saturation potential is 100 mV by absolute value for both types of junctions. Second, the mean temperature $\bar{T}$ is generally increasing with the number of measurements: from 555 to 615 K (as the maximum) for the YSZ+Pt/YSZ junction and from 560 to 580 K for the YSZ/YSZ+Pt junction. This means that the activation threshold of a junction is increasing too. Third, the reverse temperature θ is decreasing with the number of measurements: from 0.052 to 0.025 K^{-1} for the YSZ+Pt/YSZ junction and from 0.06 to 0.03 K^{-1} for the YSZ/YSZ+Pt junction. This fact is implying that the measurement is becoming less sensitive of the potential difference. In view of the second and third trends there is a worsening of the junction operation on sensing probably related to irreversible changes in the structure of constituent electrodes.

The results shown on the above pictures are consistent with the data for the samples obtained by spray pyrolysis [18] – Fig. 4. The quantities U_∞ and θ take the same values: ±100 mV and 0.04 K^{-1}, respectively, whereas the characteristic temperature differs increasing from 615 °C for dip coated samples to 630 °C for samples prepared by spray pyrolysis [6,19].

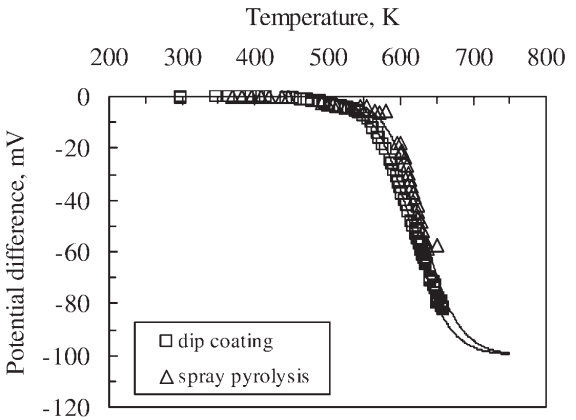

Fig. 4. Comparison of the experimental data for YSZ+Pt/YSZ junctions obtained by dip coating (measurement 2 from Fig. 3*a*) or by spray pyrolysis [18] at 4.5 mol% of Pt (measurement 3). The solid lines are fits of the data by Eq. (1)

Here we make the assumption that the two samples underwent the same changes in the course of thermal treatment despite of the different number of measurements. In other combinations of dip and spray coatings the results of comparison may worsen.

3.3. RESPONSE OF THE JUNCTION TO OXYGEN

The dependence of the potential difference of the junctions under oxygen exposure is investigated using the same experimental setup [7]. Flowing of dried air (21 % oxygen) along the sample generally causes an increase of the potential difference (by absolute value) – see Fig. 5. The initial steep increase for about 3 min is then followed by a saturation of the potential difference *U*. At the 10th minute a flow of pure nitrogen (zero oxygen) is initiated leading to a decrease of the potential difference by absolute value. This repetition of the cycles is for 3 times for checking the reproducibility of measurements. A good coincidence of the data sets is demonstrated in the figure: 2 independent measurements for the junction of YSZ/YSZ+Pt and 3 independent measurements for the junction YSZ+Pt/YSZ. All these measurements were done at a temperature (390 ± 7) °C (663 K) which is within the range of constant potential of saturation in Fig. 3 (the temperature changes do not affect the potential difference).

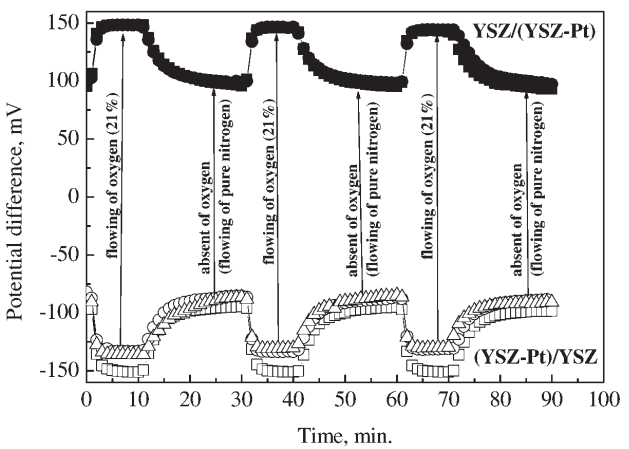

Fig. 5. Time dependence of the potential difference of the YSZ/YSZ+Pt and YSZ+Pt/YSZ junctions at circulating oxygen/nitrogen along the sample at a constant temperature. The solid lines are to guide the eye

As seen from Fig. 5, the oxygen exposure always leads to increasing of the potential difference of the YSZ/YSZ+Pt junctions. This is consistent with the basic principle of operation of a Nernstain-type oxygen sensor with an internal reference [20]. In our case, the bottom layer, which is always connected to the common electrode, plays the role of an internal reference electrode.

3.4. EFFECT OF THE PLATINUM NANOPARTICLES ON THE POTENTIAL DIFFERENCE

The oxygen transport in a dense ceramic membrane occurs on the vacancies created by yttrium. For a material to achieve high values of the ionic conductivity, one of the ways is to obtain a structure containing a large number of interconnected equivalent sites for the mobile ions. These sites are only partially occupied, if the zirconia crystal lattice is doped by yttrium [21,[22]]. The number of oxygen vacancies is then determined by the yttrium cations at the limit $\left[Y_{Zr}^{1-}\right] = 2\left[Y_0^{2+}\right] \gg n$ (Y_{Zr}^{1-} means yttrium ion in zirconium position of effective charge -1; Y_0^{2+} means a double ionized oxygen vacancy, n is the concentration of electrons). In the case of pure YSZ-ceramic layer, we expect lesser number of vacancies, which is determined only by the number of yttrium cations. Therefore, pure YSZ could be either n- or p-type depending of the oxygen pressure [22].

Another type of defects in the crystalline lattice could be introduced by the platinum nanoparticles according to the general expectation from the literature for nanopowder materials [[23]]. Then if the ceramic grains are of nanometric dimensions, the crystalline lattice should be somehow deformed. Because of the disturbances of the YSZ crystal lattice, introduced by the Pt nanoparticles, the number of oxygen vacancies increases in addition to that formed by the yttrium cations. It is shown [24] that when the distance between the atoms increases, they become to vibrate with a lower frequency and higher amplitude, respectively (at the same value of energy). Therefore, the introduction of Pt nanoparticles, which do not interact chemically with both zirconium dioxide and diffused oxygen, reduces the frequency of vibrations of the atoms. Because of the higher amplitude of vibrations of the atoms, they will easily leave their equilibrium positions thus increasing the number of oxygen vacancies in the YSZ in addition to the oxygen vacancies created by the yttrium itself. This increases the concentration of electrons in the upper electrode, for example YSZ layer (Fig. 1a), and changes the Seebeck coefficient α_i according to the equation for n–type semiconductor [25]

$$\alpha_i = \frac{k}{e}\left[2 + \ln\left(\frac{N_C^i}{n_i}\right)\right] \quad (2)$$

Here N_C^i is the conduction band density of states, k is the Boltzman's constant, e is the electron charge, n_i is the electron concentration. In Eq. (2) $i = 1$ refers to the top electrode (YSZ) while $i = 2$ refers to the bottom electrode (YSZ+Pt). Both α_i are negative, because of the sign of the dominating charge carriers (electrons). These electrons will be born by the reaction pathway $V_0^x = V_0^{2+} + 2e^-$ realized at an increasing temperature [22] (V_0^x is a neutral oxygen vacancy). However, because of the higher concentration of electrons in the bottom electrode, α_2 will become less negative than α_1 cf. Eq. (2) (see also ref. [26]). Then the potential difference ΔU, given as $\Delta U = (\alpha_1 - \alpha_2)\Delta T$, will be also negative (here ΔT is the temperature difference between the hot and cold sides of the thermocouple, composed of the junction plus the connecting wires).

Now one can understand why with increasing the temperature of YSZ+Pt/YSZ junction (Fig. 1a) the potential difference will become more negative – cf. Fig. 3a. For the junction YSZ/YSZ+Pt (Fig. 1b) the situation is reverse, i.e. with increasing the temperature the potential difference will become more positive – see Fig. 3b.

4. CONCLUSIONS

We developed a new method of impregnation of thin YSZ films with platinum nanoparticles. Ii is based on the adding of the nanoparticles prepared by a classical procedure into 8 mol% yttria-doped zirconia sol. Next supported YSZ-Pt film is prepared by dip-coating procedure to get 5.25 mol% platinum in it. This film is then used as one of the electrodes of a junction of the type YSZ+Pt/YSZ and visa versa (the second one is a pure YSZ film). Both junction structures show a good sensitivity towards oxygen in dynamic conditions that is checked by our home-build experimental setup. The latter assures on the possibility to detect with the dip-coated junctions, outlined here, also fine changes in the oxygen concentration. These findings promise the application of the obtained dip-coated junctions as the prototypes of oxygen sensors for low temperature applications in aggressive environments.

Acknowledgments. This work was supported by the grant X-1210 of the Bulgarian Fund for Scientific Investigations. The authors are thankful to Mrs. R. Todorovska from the Institute of Electronics, BAS, for the preparation of samples by spray pyrolysis and to Dr. D. Todorovsky for valuable comments on the research.

REFERENCES

1. Yamamoto, O., Y. Chujyo, K. Aoki, T. Furuichi. *Sensors Actuators B*, **13–14**, 1993, 31.
2. Yu S., Q. Wu, M. Tabib-Azar, C.-C. Liu. *Sensors Actuators B*, **85**, 2002, 212.
3. Radhakrishman, R., A. V. Virkar, S. C. Singhal, G. C. Dunhan, O. A. Marina. *Sensors Actuators B,* **105**, 2005, 312.
4. Suzuki, T., M. Kondo, K. Ogino, Y. Ishiguro, H. Takahashi. *Sensors Actuators B*, **108**, 2005, 326.
5. Dubbe, A. *Sensors Actuators B*, **88**, 2003, 138.
6. Todorovska, R., N. Petrova, D. Todorovsky. *Appl. Surface Science*, **252**, 2005, 1266.
7. Dimitrov D, Tz., C. D. Dushkin. *Centr. Eur. J. Chem.*, **3**, 2005, 605.
8. Vasylkiv, O., Y. Sakka, Y. Maeda, V. V. Skorokhod. *J. Eur. Ceramic Soc.*, **24**, 2004, 469.
9. Chen, Y.-Z., B-J. Liaw, C.-F. Kao, J.-C. Kuo. *Appl. Catalysis A*, **217**, 2001, 23.
10. Hendriks, M. G. H. M., B. A. Boukamp, J. E. Ten Eleshof, W. E. Van Zyl, H Verweij. *Solid State Ionics*, **146**, 2002, 123.
11. Peng, Z., M. Liu, E. Balko. *Sensor Actuators B*, **72**, 2001, 35.
12. Kim, J., Y. S. Lin. *J. Membrane Sci.*, **139**, 1998, 75.
13. Rampino, L. D., F. F. Nord. *J. Am. Chem. Soc.*, **63**, 1942, 2745.
14. Devi, G. S., V. J. Rao. *Bull. Mater. Sci.*, **23**, 2000, 467 (India).
15. Henglein, A., B. G. Ershov, M. Malow. *J. Phys. Chem.*, **99**, 1995, 4129.
16. Ahmadi, T. S., Z. L. Wang, T. C. Green, A. Henglein. M. A. El-Sayed. *Science*, **272**, 1996, 1924.
17. Dushkin, C., S. Stoianov, A. Bojinova, S. Russev. *Ann. Univ. Sofia, Fac Chim*., in press.
18. Dimitrov, D. Tz., C. D. Dushkin, N. L. Petrova, R. V. Todorovska, D. S. Todorovsky, S. Y. Anastasova, D. H. Oliver. *Sensors Actuators A*, in press.
19. Petrova, N., R. Todorovska, D. Todorovsky, D. Shopova. *Key Eng. Mater.,* **264–268**, 2004, 427.
20. Van Setten, E., T. M. Gur, D. H. A. Blank, J. C. Bravman, M. R. Beasley. *Rev. Sci. Instrum*., **73**, 2002, 156.
21. Kilner, J. A. *Solid State Ionics*, **129**, 2000, 3.
22. Kofstad, P. Nonstoichiometry, Diffusion and Electrical Conductivity in Binary Metal Oxides. New York, 1972 (Russian Edition).
23. Polyakov, A. A., Technology of the Ceramic Radio-Electronic Materials. Moscow, 1989, (in Russian).
24. Landau, L. D., E. M. Lifshitz, Theoretical Physics, vol. 5, Moscow, 1995 (in Russian).
25. Antipov, B. L., V. S. Sorokin, V. A. Terehov, Problems in Materials for the Electronic Devices. Moscow, 1990 (in Russian).
26. Bonch-Bruevich, V. L., S. G. Kalashnikov, The Physics of Semiconductors, Moscow, 1990 (in Russian).

Received December 2006

Dimitre Dimitrov
St. Kliment Ohridski University of Sofia
Faculty of Chemistry
Department of General and Inorganic Chemistry
1, James Bourchier Blvd.
1164 Sofia, Bulgaria
E-mail: DTsenov@wmail.chem.uni-sofia.bg